Bulletin of Geophysics and Oceanography Vol. 67, n. 2, pp. 277-294; June 2026
DOI 10.4430/bgo00528

Seismo-magmatic interaction and stress evolution during the 2020–2024 Reykjanes Rift cycle, Iceland

A. Figlioli[1], A. D'Alessandro[2], R. Martorana[2,3] and M. Guastella[4]

[1] *Istituto Nazionale di Geofisica e Vulcanologia, Sezione di Milano, Milan, Italy*
[2] *Istituto Nazionale di Geofisica e Vulcanologia, Osservatorio Nazionale Terremoti, Rome, Italy*
[3] *Dipartimento di Scienze della Terra e del Mare, Università degli Studi, Palermo, Italy*
[4] *Dipartimento di Ingegneria, Civile, Edile e Ambientale, Università di Roma La Sapienza, Rome, Italy*

(Received: 31 October 2025; accepted: 17 February 2026; published online: 15 April 2026)

ABSTRACT Between 2020 and 2024, the Reykjanes Peninsula (Iceland) experienced a renewed phase of seismic and volcanic unrest after several centuries of relative quiescence. Four eruptive episodes occurred within the Fagradalsfjall–Sundhnúksgígar volcanic system, each associated with pronounced seismic swarms and significant changes in the spatial and temporal distribution of earthquake activity. In this study, we analyse the seismicity recorded during this period using a homogeneous earthquake catalogue provided by the Icelandic Met Office, with the aim of characterising the evolution of seismic activity in relation to the eruptive sequence. The results document systematic temporal variations in seismicity rate, cumulative seismic energy release, and *b*-value, as well as a progressive NE-ward migration of seismic clusters along the rift system. Seismicity evolves from relatively deep and spatially distributed activity to shallower and more localised fracturing in temporal proximity to eruptive onsets. While *b*-value decreases are not uniquely associated with eruptions, their temporal fluctuations are consistent with recurrent changes in the seismic regime during phases of volcanic unrest. The observed patterns are interpreted within the framework of previously published geophysical and geodetic studies, which indicate a multi-level magmatic plumbing system beneath the Reykjanes Peninsula. Our results suggest that seismicity provides indirect constraints on the evolving stress conditions and magma transport pathways during the 2020–2024 unrest, highlighting the strong interaction between tectonic extension and magmatic processes in an active rift environment. This study contributes to a refined seismological characterisation of rifting-related volcanic unrest and provides observational benchmarks for future multidisciplinary investigations of seismo-magmatic coupling.

Key words: Reykjanes Peninsula, Fagradalsfjall volcanic system, *b*-value variation, stress accumulation, magmatic migration, active rifting Iceland.

1. Introduction

In recent years, the Reykjanes Peninsula, located in the south-western part of Iceland, has once again become one of the most significant natural laboratories for studying the interaction between tectonic and magmatic processes within an oblique rift environment.

After more than eight centuries of quiescence, the Fagradalsfjall volcanic system produced a sequence of effusive eruptions (2021, 2022, 2023, and 2024), each preceded by intense seismic swarms and broad crustal deformation (Fischer *et al.*, 2022; Sigmundsson *et al.*, 2022; Parks *et al.*, 2023; Matthews *et al.*, 2024). This exceptional sequence provided a unique opportunity to investigate the relationships among tectonic stress accumulation, fluid migration, and magma intrusion, and to evaluate the effectiveness of seismological parameters, particularly the Gutenberg–Richter *b*-value, as indicators of stress variation preceding eruptive activity.

The overall geodynamic framework of Iceland (Fig. 1) highlights the Reykjanes Peninsula as the transition zone between the oceanic ridge system and the continental crust influenced by the Iceland mantle plume.

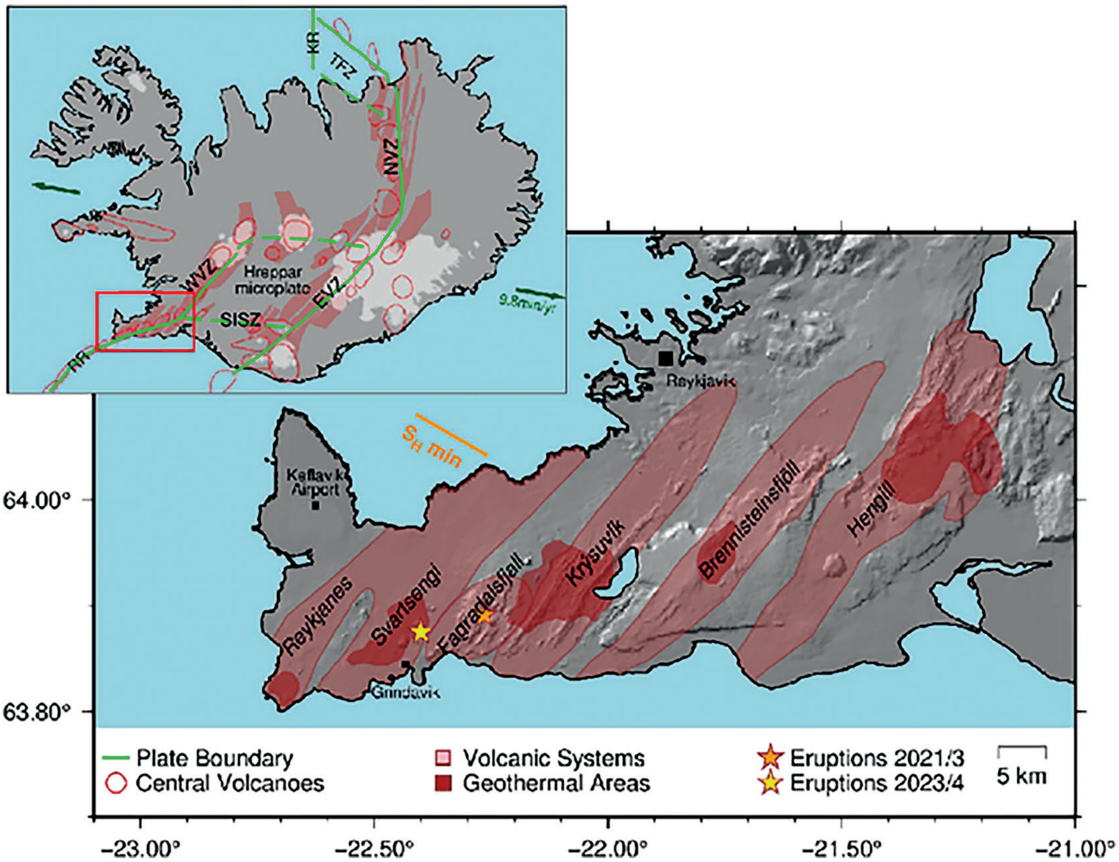

Fig. 1 - Geodynamic framework of Iceland and location of the Reykjanes Peninsula (modified after Jenkins *et al.*, 2025). The map shows the Mid-Atlantic Ridge (green dashed line), the main Icelandic volcanic systems, and the crust–mantle boundary derived from seismic imaging. The study area (black rectangle) highlights the Fagradalsfjall system. Acronyms in the inset: RR = Reykjanes Ridge; WVR = Western Volcanic Rift; EVZ = Eastern Volcanic Zone; NVZ = Northern Volcanic Zone; SISZ = South Iceland Seismic Zone; TFZ = Tjörnes Fracture Zone; KR = Kolbeinsey Ridge.

The recent activity of the Fagradalsfjall volcano-tectonic system has been characterised by four major eruptive episodes between 2021 and 2024 (Fig. 2), each preceded by intense seismic swarms:

- the Geldingadalir 2021 eruption – Initiated on 19 March 2021 following a seismic swarm of more than 30,000 events culminating in the *M* 5.3 mainshock on 24 February. The intrusion of a ~9 km-long dike was followed by a rapid decrease in seismicity and deformation in the days immediately preceding vent opening (Sigmundsson *et al*., 2022; Hrubcová *et al*., 2025);

- the Meradalir 2022 eruption – Began on 3 August 2022, preceded by renewed seismic activity and a dike intrusion with a shallow top (~1 km) and an estimated injection rate of ~49 m³/s (Parks *et al*., 2023);
- the Litli Hrútur 2023 eruption – Occurred on 10 July 2023 farther NE, associated with shallow seismicity consistent with the activation of an eruptive conduit fed by magma reservoirs at 7–9 km depth (Matthews *et al*., 2024);
- the Sundhnúksgígar 2023–2024 eruptions – A sequence of events between December 2023 and February 2024 in the Svartsengi area, linked to a dynamic, multi-reservoir magmatic domain in the mid-crust, hydraulically connected to the Fagradalsfjall system (Marshall *et al*., 2024; Matthews *et al*., 2024).

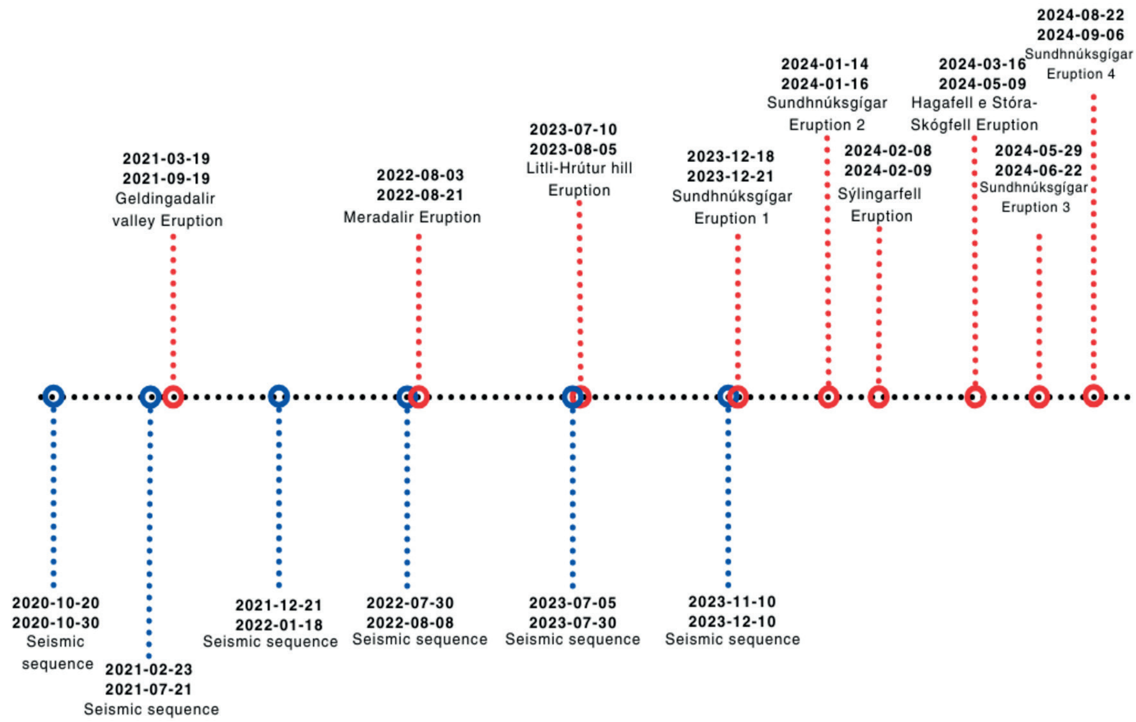

Fig. 2 - Seismo-eruptive timeline of the Fagradalsfjall volcanic system (2020–2024). Major seismic sequences are shown in blue and volcanic eruptions in red. The four main episodes (Geldingadalir 2021, Meradalir 2022, Litli Hrútur 2023, and Sundhnúksgígar 2023–2024) are labelled as Eruptions. The progressive shortening of the interval between seismic crises and eruptions highlights the increasing dynamism of the magmatic system.

The seismicity accompanying the Reykjanes eruptive episodes exhibits a wide variety of focal mechanisms, including events with significant non-double-couple (non-DC) components, reflecting changes in fluid pressure and mixed tensile–compressive fracturing processes (Hrubcová *et al*., 2025).

Recent studies have shown that temporal variations in the *b*-value can indicate local changes in the stress state and in the relative proportion of small-to-large earthquakes, potentially related to dike propagation or magma degassing (Murru *et al*., 2007; Gulia and Wiemer, 2010; Gulia *et al*., 2018).

Based on a dataset of more than 50,000 events recorded between 2020 and 2024 by the Icelandic Met Office (IMO), this study aims to assess the potential of the *b*-value as a precursor indicator of eruptive activity within the Fagradalsfjall system. The analysis combines spatial, temporal, and depth distributions of seismicity with eruptive timelines to identify systematic patterns in *b*-value evolution preceding and accompanying major eruptive episodes.

This study provides a quantitative seismological perspective on the 2020–2024 unrest cycle of the Fagradalsfjall–Sundhnúksgígar volcanic system by systematically analysing the temporal evolution of seismicity rate, released energy, and *b*-value variations over the entire rifting sequence. Unlike previous works that focused on individual eruptive episodes or relied primarily on geodetic observations, this contribution offers a unified, catalogue-based analysis spanning multiple eruptions and pre-eruptive phases. The main outcome of the study is the identification of recurrent seismic patterns preceding eruptive onsets, which are discussed as consistent with time-dependent changes in the crustal stress regime and magma transport processes inferred from independent geophysical studies. These results highlight the potential of long-term seismic catalogues to provide valuable constraints on the timing and evolution of volcano-tectonic unrest, while explicitly acknowledging the need for multidisciplinary integration to fully resolve the underlying physical mechanisms.

2. Geological and geophysical setting

The Reykjanes Peninsula forms the westernmost onshore segment of the Icelandic Rift system and represents the only subaerial exposure of the Mid-Atlantic Ridge (Einarsson, 2008; Sigmundsson *et al*., 2022). It extends for approximately 50 km in a NE–SW direction between the Reykjanes Peninsula tip and Faxaflói bay, comprising a series of aligned volcanic systems including Reykjanes, Svartsengi, Krýsuvík, Brennisteinsfjöll, and Bláfjöll (Jenkins *et al*., 2025). This region marks the transition between the oceanic portion of the ridge and the continental crust influenced by the Icelandic mantle plume, generating a complex oblique-extensional regime that controls the peninsula's volcano-tectonic activity.

Geologically, the peninsula consists of Pleistocene to Holocene tholeiitic and olivine basalts, produced by linear fissure eruptions typical of Icelandic rift zones (Hakim *et al*., 2024). The exposed formations include basaltic lava flows, hyaloclastite breccias, and tuffs younger than 0.8 Myr (Jenkins *et al*., 2025).

The Fagradalsfjall area, located in the central part of the peninsula, is characterised by an active rift zone approximately 5–7 km wide, bounded by high-angle normal faults and subvertical NE–SW dike swarms, consistent with the regional extension direction (Hrubcová *et al*., 2025).

The regional deformation pattern is governed by an oblique transtensional stress regime, with an average extension rate of 19 mm/yr and a dominant right-lateral component along the WSW–ENE faults (Einarsson, 1991; Clifton and Katternhorn, 2006; Büyükakpınar *et al*., 2025). This configuration promotes the formation of pull-apart basins and the propagation of shallow magmatic intrusions, often accompanied by intense swarm-type seismicity (Fischer *et al*., 2022).

Focal mechanism studies have revealed numerous events with significant non-DC components, attributed to variations in magmatic fluid pressure and mixed tensile–compressive fracturing processes (Hrubcová *et al*., 2025). Seismic and magnetotelluric investigations (Jenkins *et al*., 2025) indicate that the crust beneath the Reykjanes Peninsula is 18–21 km thick, with the brittle-ductile transition located at 6–8 km depth (Mackenzie *et al*., 1982, Darbyshire *et al*., 2000; Hrubcová *et al*., 2025). A low-velocity, high-conductivity anomaly beneath the Fagradalsfjall area has been interpreted as a mid-crustal magmatic domain, acting as an intermediate reservoir between the Moho and shallow intrusions (Matthews *et al*., 2024). Petrological and geochemical analyses of the 2021–2024 eruptions suggest that the system is fed by multiple, compositionally distinct magma reservoirs (Halldórsson *et al*., 2022; Marshall *et al*., 2024). This multilevel plumbing system, located at depths of 7–9 km, explains both the isotopic variability of erupted lavas and the progressive NE-ward migration of eruptive vents over time (Jenkins *et al*., 2025).

The schematic cross-section of the Fagradalsfjall volcanic system shown in Fig. 3 illustrates the first-order structural and magmatic features inferred from previous geophysical and volcanological studies and from the seismicity patterns analysed in this work. The conceptual model depicts subvertical NE–SW–oriented dike intrusions associated with the eruptive activity between 2021 and 2024, a mid-crustal magma storage region located at approximately 7–9 km depth and hydraulically connected to a deeper magmatic source near the Moho at about 15–20 km depth, and the brittle-ductile transition separating the seismically active upper crust from the underlying ductile domain. The architecture of the rift is defined by the coexistence of normal and strike-slip faults consistent with a transtensional stress regime, and the model also indicates the surface locations of the four main eruptive centres, namely Geldingadalir (2021), Meradalir (2022), Litli Hrútur (2023), and Sundhnúksgígar (2023–2024).

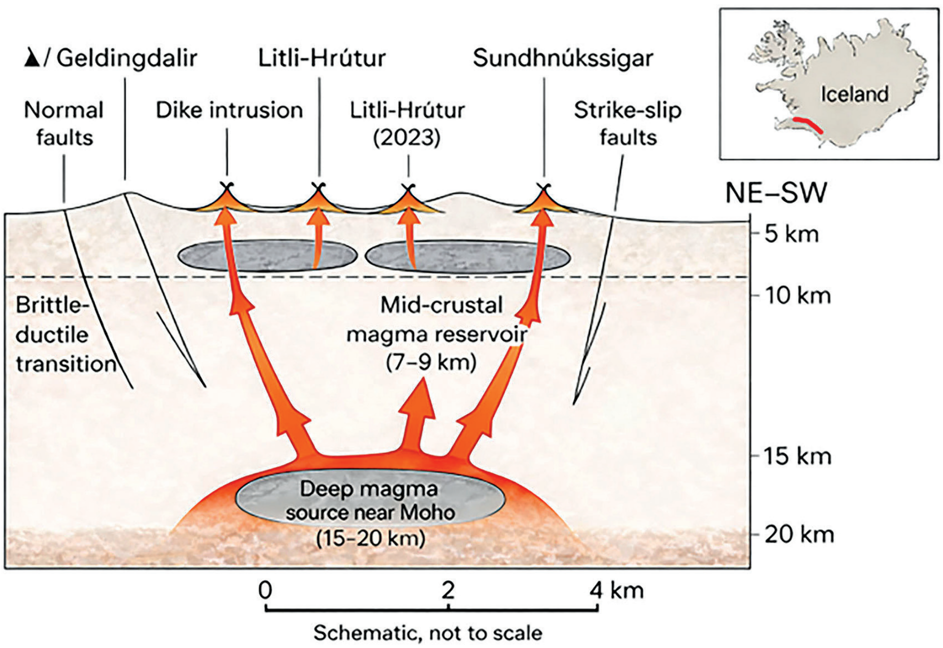

Fig. 3 - Schematic NW–SE cross-section of the Fagradalsfjall–Sundhnúksgígar volcanic system illustrating the main structural and magmatic elements inferred from published geophysical, geodetic, and petrological studies. The diagram shows a mid-crustal magma reservoir located at approximately 7–9 km depth and a deeper magma source near the Moho at about 15–20 km depth, together with subvertical dike intrusions feeding the surface eruptive centres of Geldingadalir, Litli Hrútur, and Sundhnúksgígar. Normal and strike-slip faults outline the transtensional rift architecture, while the brittle-ductile transition is indicated schematically. Red arrows represent conceptual magma ascent paths from the deep magma source towards the mid-crustal reservoir and surface vents. Depths, geometries, and volumes are schematic and not to scale; the figure is intended as a conceptual framework integrating seismic observations with independent geophysical models, rather than as a quantitative depth-constrained model.

The IMO operates the primary volcano-tectonic monitoring network in the area, combining broadband and accelerometric instruments with high temporal resolution (Jonsdottir *et al.*, 2021).

The local REYKJANET network, comprising more than 25 seismic stations distributed between Reykjanes, Krýsuvík, and Fagradalsfjall, provides hypocentral uncertainties below 1 km for shallow events (< 10 km) and enables the accurate determination of magnitude and focal mechanisms even for low-energy earthquakes (Parks *et al.*, 2023).

Continuous global navigation satellite system (GNSS) and interferometric synthetic aperture radar (InSAR) measurements complement the seismic data, enabling detailed mapping of crustal deformation. The improved combined scatterer interferometry with optimised point scatterers technique (Hakim *et al.*, 2024) achieved sub-centimetric precision during the 2021 unrest, with a root-mean-square error of only 0.6 cm relative to GNSS data.

The seismic dataset analysed in this study provides the primary basis for the investigation of temporal variations in seismicity and *b*-value during the 2020–2024 eruptive sequence. Published geodetic observations (GNSS and InSAR) are used here to provide an independent contextual framework for the interpretation of the seismic results, rather than being directly analysed.

The seismicity shown in Fig. 4 is derived from the earthquake catalogue provided by the IMO. The dataset covers the period from January 2020 to February 2024 and includes earthquakes

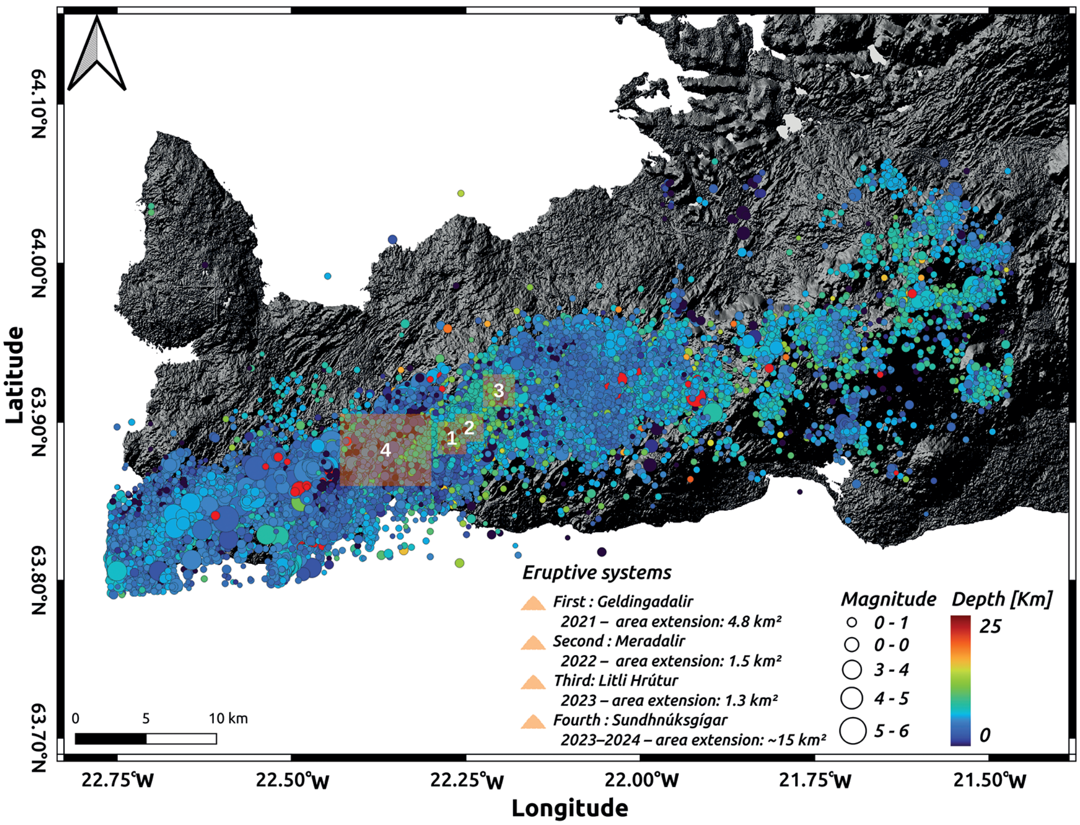

Fig. 4 - Spatial and depth distribution of seismicity in the Reykjanes Peninsula between 2020 and 2024 (IMO catalogue). Circle colour indicates focal depth and circle size is proportional to earthquake magnitude. The dominance of shallow events (< 10 km) and the NE-ward migration of clusters coincide with the eruptive centres of Geldingadalir, Meradalir, Litli Hrútur, and Sundhnúksgígar.

across the Reykjanes Peninsula recorded by the permanent seismic monitoring network. Event locations and magnitudes are determined using the operational IMO procedures, while details on catalogue processing and statistical analysis are described in Section 3. The seismicity recorded between 2020 and 2024 exhibits spatial and depth-dependent variations along the NE–SW trend of the Fagradalsfjall system. While a systematic space–time migration is not directly imaged by the figures presented here, the observed distribution of seismic clusters and their temporal succession are consistent with an along-axis evolution of seismic activity.

The seismicity–depth distribution shown in Fig. 4 indicates that most earthquakes are concentrated within the upper ~10 km of the crust, with a pronounced density maximum between approximately 4 and 8 km depth. This depth range is commonly interpreted, based on seismicity patterns and independent geophysical constraints, as corresponding to the brittle-ductile transition beneath the Fagradalsfjall system.

Deeper events (down to ~20 km) occur beneath the Svartsengi area, indicating a structural and magmatic connection between the deep source and the upper crustal storage levels. Epicentral alignment follows NE–SW trends parallel to the main rift structures, confirming the strong structural control of faulting and diking on the spatial distribution of seismic activity.

3. Methods

The seismic dataset analysed in this study was retrieved from the IMO database (IMO, n.d.), covering the period September 2020 to January 2024. The catalogue contains more than 50,000 events spanning the magnitude range reported by the IMO for the study area. This time window encompasses the major seismic crises and eruptive episodes affecting the Fagradalsfjall system during the recent unrest cycle (Geldingadalir 2021; Meradalir 2022; Litli Hrútur 2023; Sundhnúksgígar 2023–2024). The Gutenberg–Richter (GR) law (Gutenberg and Richter, 1944) represents one of the fundamental empirical relationships in seismology, describing the statistical distribution of earthquake magnitudes within a given region or catalogue. It is expressed as:

$$log_{10} N = a - bM \quad (1)$$

where N is the cumulative number of earthquakes with magnitude larger than, or equal to, magnitude M and a and b are region-specific constants. The b-value expresses the relative proportion between small and large events, while a reflects the seismic productivity of the region. Typical b-values range between ~0.8 and 1.2 in most tectonic environments.

The GR law provides the statistical framework for characterising earthquake magnitude–frequency distributions and estimating temporal variations in earthquake occurrence rates. Variations in the b-value derived from this relationship are widely used to characterise changes in the seismic regime. The reliability of the b-value estimation, however, critically depends on three factors: catalogue completeness, declustering of dependent events, and statistical fitting method used.

Determining the magnitude of completeness (M_c), defined as the lowest magnitude above which the catalogue is considered complete, is a prerequisite for reliable b-value estimation. M_c was initially estimated using the Maximum Curvature (MAXC) method (Wiemer and Wyss, 2000) as a preliminary and computationally efficient approach. This initial estimate was subsequently refined using a stability analysis of the b-value to ensure temporal robustness and consistency across the study period. Only earthquakes with magnitudes equal to, or greater than, the final selected M_c were retained for the *b*-value analysis. This method detects the magnitude corresponding to the point of maximum curvature in the cumulative frequency–magnitude distribution, marking the transition between incomplete and complete portions of the catalogue.

However, completeness may vary during periods of intense seismic activity. Since network performance and detection thresholds may vary through time, especially during high-activity phases, the *b*-positive method (van der Elst, 2021) was adopted to mitigate incompleteness effects. This robust estimator enables reliable computation of the *b*-value even when small events are missing or catalogue coverage is non-stationary. Unlike classical GR fitting, which may bias results when low-magnitude events are underdetected, the *b*-positive method relies on magnitude differences between pairs of earthquakes, minimising sensitivity to incomplete sampling.

Earthquake catalogues often contain numerous dependent events (foreshocks, aftershocks, swarms), which can bias statistical analyses if not properly filtered. To isolate independent background seismicity, the Gardner–Knopoff algorithm (Gardner and Knopoff, 1974) was employed. This classical approach defines a magnitude-dependent space–time window around each event. The largest earthquake in the window is classified as the mainshock, while all subsequent events within such window are identified as dependent (aftershocks). Events outside any space–time window are retained as independent background events.

Alternative window parameterisations such as those of Gruenthal (van Stiphout *et al*., 2012) and Uhrhammer (1986) were tested for sensitivity, though the Gardner–Knopoff approach was ultimately preferred for its stability and reproducibility in the Reykjanes dataset.

The declustering procedure was implemented deterministically by ordering events by decreasing magnitude and applying magnitude-dependent space–time windows. For each event, a magnitude-dependent spatial and temporal window, within which neighbouring earthquakes are evaluated, is, then, defined. The largest event inside each window is identified as the mainshock, whereas the remaining events falling within the associated space–time domain are classified as dependent events. This procedure is iteratively applied until all earthquakes in the catalogue are either assigned to a mainshock cluster or classified as background seismicity. This method, while simple, effectively reduces the influence of clustering, ensuring that subsequent *b*-value estimations reflect genuine background stress variations rather than short-term aftershock sequences.

Hypocentral location uncertainties vary as a function of depth and network geometry. For earthquakes shallower than 10 km, the dense REYKJANET network ensures typical horizontal and vertical location errors lower than approximately 1 km, consistent with previous assessments (Parks *et al*., 2023). At greater depths, location uncertainties progressively increase due to reduced ray coverage and increased sensitivity to the adopted velocity model. Consequently, earthquakes deeper than 10 km are interpreted primarily in terms of their overall depth distribution and first-order spatial patterns, rather than precise hypocentral positioning.

This workflow (Fig. 5) ensures that temporal variations in the *b*-value reflect genuine changes in seismic regime rather than artefacts related to catalogue incompleteness or clustering. The process begins with the acquisition of the IMO catalogue, followed by declustering using the Gardner–Knopoff algorithm to isolate background events. Subsequently, M_c is estimated using the MAXC method, ensuring that only complete portions of the catalogue are included in the computation of the *b*-value, which is, then, determined through the *b*-positive method. Finally, the temporal evolution of the *b*-value is correlated with eruptive activity and cumulative seismic energy release over the 2020–2024 period. The combination of declustering, completeness estimation, and robust *b*-value computation provides a statistically consistent approach to quantifying stress evolution and magmatic processes on the Reykjanes Peninsula. This workflow ensures that temporal changes in the *b*-value are physically meaningful, ensuring that temporal variations in the *b*-value reflect genuine changes in seismic regime rather than artefacts related to catalogue incompleteness or clustering.

4. Data analysis and results

The analysis of the IMO seismic catalogue from September 2020 to January 2024 reveals a clear temporal correlation between seismic crises and eruptive phases within the Fagradalsfjall volcanic system. As illustrated in Fig. 2, each eruptive episode (2021, 2022, 2023, and 2023–2024) was preceded by a sharp increase in seismic activity, followed by an abrupt drop immediately after the onset of the eruptions. This behaviour is consistent with the dike propagation and pressurisation model described by Sigmundsson *et al*. (2022) and Parks *et al*. (2023), where seismicity accelerates during dike emplacement and declines once magma is released to the surface.

The overall time evolution delineates four main phases:

1. 2020–early 2021: widespread and relatively deep seismicity (down to 15 km) associated with crustal recharge processes;
2. March 2021: intense seismic crisis culminating in the Geldingadalir eruption, with more than 30,000 events and a maximum magnitude *M* 5.3;
3. 2022–2023: progressive NE-ward migration of activity related to smaller intrusions [Meradalir, 2022 and Litli Hrútur, 2023: Jenkins *et al*. (2025)];
4. late 2023–early 2024: a more complex phase with multiple intrusions and four distinct eruptions at Sundhnúksgígar, indicating a mature and interconnected magmatic system (Marshall *et al*., 2024; Matthews *et al*., 2024).

This trend demonstrates a systematic NE-ward propagation of the feeding zone and a decreasing recurrence interval between seismic and eruptive phases, consistent with the evolution from a closed magmatic system towards a more open, hydraulically connected configuration (Fischer *et al*., 2022).

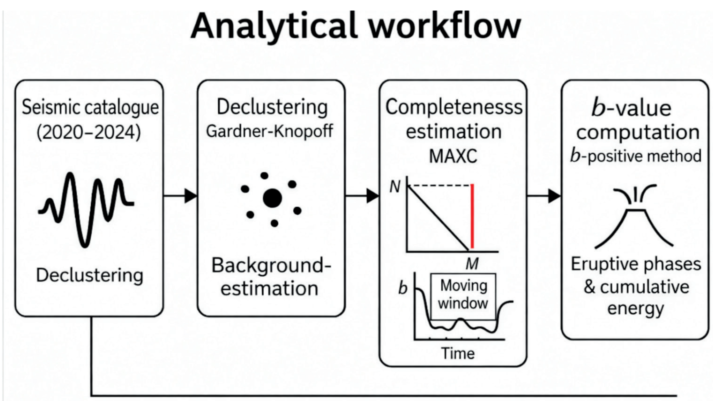

Fig. 5 - Analytical workflow of the study. The flowchart summarises the main steps of the analysis: 1) acquisition of seismic data from the IMO catalogue (2020–2024), 2) declustering using the Gardner–Knopoff algorithm, 3) estimation of magnitude of completeness M_c via the MAXC method, 4) computation of the *b*-value using the *b*-positive approach, and 5) correlation with eruptive phases and cumulative energy release.

Fig. 6 illustrates the temporal evolution of cumulative seismicity, released seismic energy, and *b*-value variations during the study period. The spatial organisation and clustering of seismicity are shown separately in Fig. 4, which provides the complementary spatial context for the temporal patterns discussed here.

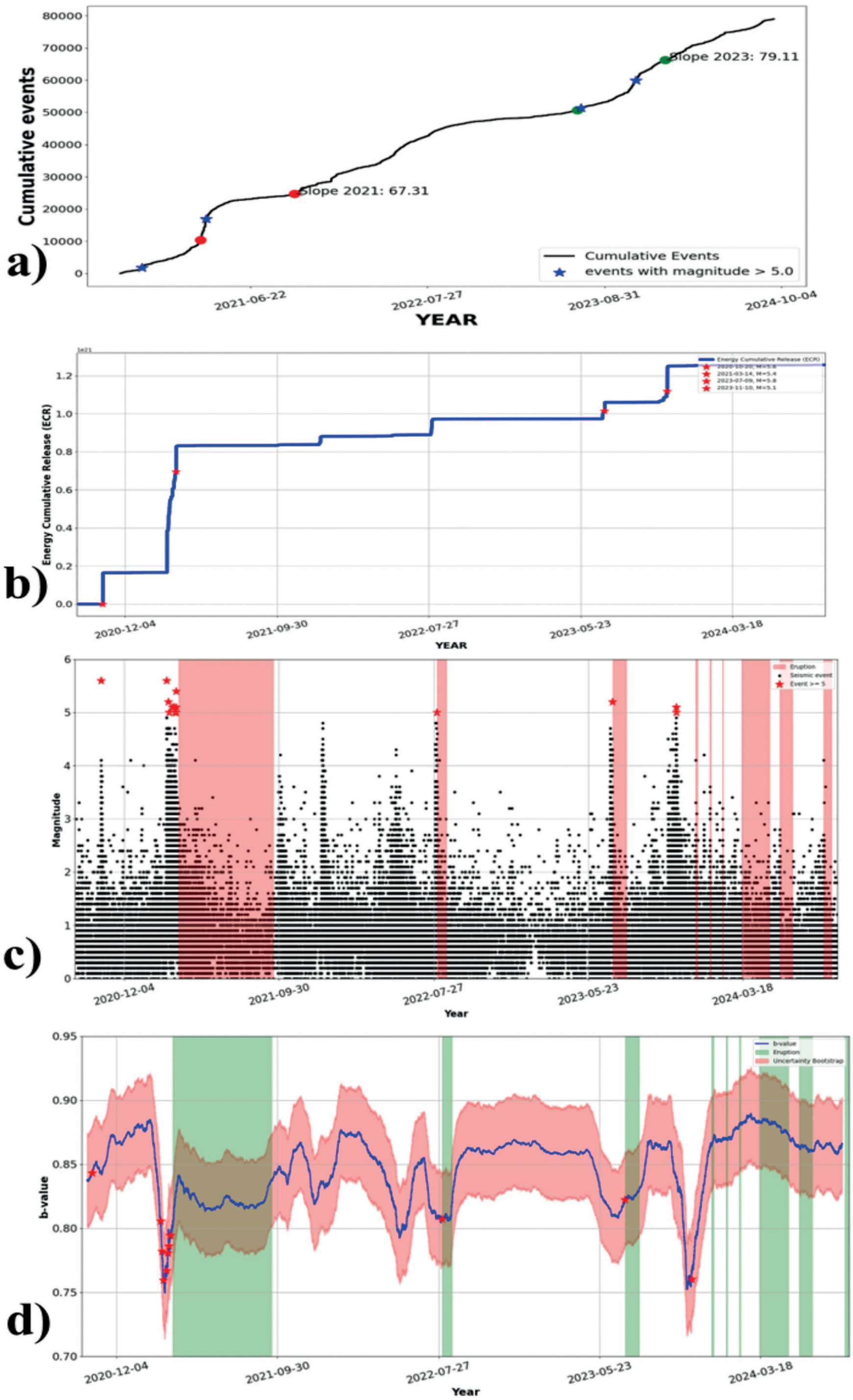

Fig. 6 - Seismic activity panel for the 2020–2024 Reykjanes cycle: a) cumulative number of earthquakes; b) cumulative seismic energy release; c) temporal distribution of earthquake magnitudes; d) temporal evolution of the *b*-value with bootstrap uncertainty. Green shaded areas mark eruptive periods; red stars mark the largest events ($M > 5$). Local minima in the *b*-value precede eruptive episodes, suggesting a link between stress accumulation and magma intrusion.

The cumulative number of earthquakes exhibits a distinctly nonlinear temporal evolution, characterised by step-like increases that mark the occurrence of major seismic crises. Similarly, the cumulative seismic energy release displays an impulsive pattern, with sharp energy increments associated with the main dike intrusion episodes identified in March 2021, August 2022, July 2023, and December 2023. In addition, peaks in cumulative energy release are temporally synchronised with local minima in the *b*-value, suggesting an increase in differential stress conditions in the period preceding eruptive activity. A comparative examination of the time-aligned figures (Figs. 2 and 6) reveals systematic temporal relationships between seismicity rate, energy release, and eruptive onsets throughout the 2020–2024 Reykjanes cycle (Table 1).

Table 1 - Qualitative summary of the temporal relationships between seismic parameters (seismic rate, cumulative energy, and *b*-value) and the main eruptive episodes of the 2020–2024 Reykjanes cycle, as derived from Figs. 2 and 6. Arrows indicate increasing (↑), decreasing (↓) or strong (↑↑) multiple increasing trends. The observed patterns show that each eruptive phase was preceded by an acceleration in seismicity and energy release, accompanied by a decrease in *b*-value, consistent with progressive stress loading and magma pressurisation in the crust.

Eruptive episode	**Seismic rate**	**Cumulative energy**	***b*-value trend (Fig. 6d)**	**Depth range / migration**	**Interpretation**
Geldingadalir (2021)	↑ before eruption	↑ stepwise	↓ marked minimum pre-eruption, ↑ post-eruption	4–8 km (main cluster)	Opening of the magmatic system; first connection between deep and shallow reservoirs
Meradalir (2022)	↑ moderate	↑ slight	↓ small decrease	4–8 km, shifting NE	Minor intrusion with limited stress accumulation
Litli Hrútur (2023)	↑ strong	↑↑ significant	↓ pronounced minimum (~0.75), ↑ after onset	4–10 km, migrating NE	Enhanced pressurisation and dike propagation
Sundhnúksgígar (2023–2024)	↑↑ multiple peaks	↑↑ multiple surges	↓ persistent low (~0.7)	0–15 km, overlapping clusters	Mature interconnected plumbing system with multi-reservoir behaviour

Each eruptive phase is preceded by a marked increase in earthquake rate and cumulative energy, followed by a rapid decay after eruption onset. The temporal evolution of the *b*-value (Fig. 6d) shows multiple local minima throughout the study period. Several of these minima occur in temporal proximity to eruptive onsets, whereas others are not directly followed by surface eruptions. In particular, two pronounced *b*-value decreases observed between September 2021 and July 2022 are not associated with eruptive activity. These features indicate that *b*-value minima do not uniquely correspond to eruption triggering, but may also reflect transient stress perturbations, magma redistribution, or aborted intrusions that do not culminate in surface eruptions. This behaviour suggests that the *b*-value varies inversely with stress accumulation, being sensitive to periods of crustal loading and dike propagation, while its post-eruptive increase is consistent with a relaxation of the stress field following magma discharge.

Such qualitative patterns are visually evident from the multi-panel seismic activity plot (Figs. 6a to 6d) and are consistent with interpretations proposed by Sigmundsson *et al*. (2022), Marshall *et al*. (2024), Matthews *et al*. (2024), and Hrubcová *et al*. (2025). The observations also confirm the NE-ward migration of active zones (Figs. 2 and 4), as inferred from the spatio-temporal evolution of seismic clusters, suggesting progressive reorganisation of the magmatic plumbing system and increasing hydraulic connectivity among eruptive centres.

The cumulative energy curve reaches its largest increments during the 2021 crisis and again during the 2023–2024 sequence, suggesting two principal phases of magmatic overpressure and tectonic stress release. This pattern aligns with the interpretation of Hrubcová *et al*. (2025), who attributed the Reykjanes Peninsula's seismic variability to cyclic phases of stress accumulation and release in response to episodic pressurisation of mid-crustal magma storage zones.

The spatial distribution of hypocentres (Fig. 4) delineates a well-defined NE–SW-oriented seismic belt, parallel to the regional extensional direction of the Mid-Atlantic Ridge. Most events are concentrated between 4 and 8 km depth, coinciding with the brittle–ductile transition and the location of mid-crustal magma reservoirs shown in the schematic cross-section (Fig. 3). Deeper earthquakes (10–20 km) occur beneath the Svartsengi area, probably reflecting feeding processes from the deep magma source near the Moho, as proposed by Marshall *et al*. (2024) and Matthews *et al*. (2024). It should be noted that, while the presence of seismicity at depths greater than 10 km provides qualitative constraints on the vertical extent of the active system and is consistent with a deeper magmatic source, the exact depths of these events are affected by larger location uncertainties and should, therefore, be interpreted with caution. Spatially, the 2021–2022 clusters are confined to the south-western sector (Geldingadalir–Meradalir), while later crises (2023–2024) migrated NE-ward towards Litli Hrútur and Sundhnúksgígar. This lateral propagation of seismicity is consistent with the geodetic evidence for northward displacement of crustal uplift centres (Hakim *et al*., 2024) and supports a scenario of stepwise dike migration along an evolving fissure swarm.

The analysis of the four main seismic sequences shown in Fig. 4, together with the additional seismic cluster maps, reveals the presence of spatially distinct domains within the Fagradalsfjall volcanic system. The 2021 sequence is characterised by a compact cluster located near the Geldingadalir eruptive centre, with hypocentres mainly concentrated between 6 and 8 km depth. In 2022, seismicity migrated towards the Meradalir area, forming a smaller and shallower cluster dominated by events consistent with vertical dike propagation. The 2023 sequence associated with the Litli Hrútur eruption exhibits a broader and more fragmented spatial distribution, extending down to approximately 10 km depth. Finally, the 2023–2024 activity beneath the Svartsengi–Sundhnúksgígar area is characterised by multiple overlapping seismic clusters spanning a wide depth range, from near-surface levels down to about 15 km. Taken together, the spatial evolution of these clusters outlines a progressive NE-ward migration of seismicity, suggesting the activation of a fracture corridor connecting the different eruptive centres along the Reykjanes fissure zone (Jenkins *et al*., 2025). This pattern agrees with Büyükakpınar *et al*. (2025) and Hrubcová *et al*. (2025), who described the region as a transtensional domain where dike intrusions propagate along NE–SW oblique faults accommodating both extensional and shear components.

The temporal evolution of the *b*-value shown in Fig. 6d is characterised by pronounced oscillations throughout the 2020–2024 period. In particular, a sequence of systematic *b*-value minima is observed in temporal proximity to the onset of the main eruptive phases. Prior to the 2021 Geldingadalir eruption, the *b*-value decreases from approximately 0.95 to 0.78 during March 2021. A similar reduction, reaching values close to 0.8, accompanies the

August 2022 Meradalir intrusion. An even more pronounced decrease, down to about 0.75, precedes the July 2023 Litli Hrútur eruptive crisis. Finally, during the 2023–2024 activity at Sundhnúksgígar, the *b*-value further declines to values around 0.7 between December 2023 and February 2024.

These variations, statistically significant relative to the bootstrap uncertainty (± 0.05), indicate a robust correlation between low *b*-values and phases of elevated differential stress during dike propagation and magma accumulation, while higher values are consistent with post-eruptive stress relaxation. Such behaviour aligns with the findings of Murru *et al*. (2007) and Gulia *et al*. (2018), confirming the *b*-value as a sensitive proxy for stress evolution.

In the Icelandic context, these results indicate a recurrent magmatic–stress cycle, in agreement with the multi-reservoir model proposed by Marshall *et al*. (2024) and Matthews *et al*. (2024).

5. Discussion

The seismic observations presented in this study reveal systematic temporal and spatial patterns during the 2020–2024 unrest cycle of the Reykjanes Peninsula. These patterns are interpreted here within the context of published geophysical and geodetic studies, which provide independent constraints on magma storage and deformation processes. The seismic activity recorded across the Reykjanes Peninsula between 2020 and 2024 is consistent with recurrent phases of seismic activation and quiescence within the upper crust, as documented by the temporal evolution of seismicity rate, cumulative energy release, and *b*-value variations.

Temporal variations in the *b*-value (Fig. 6d) show systematic minima in temporal proximity to intense seismicity and to the onset of eruptive phases. Although the *b*-value is not a direct measure of stress, its temporal variability is widely used to characterise changes in seismic regime. In the Reykjanes dataset, lower values are observed during phases of intense seismicity and dike propagation, whereas higher values follow eruptive onsets, consistent with a transition toward stress relaxation and a modified rupture population.

These interpretations are consistent with previous studies discussing the stress sensitivity of *b*-value variations (e.g. Murru *et al*., 2007; Gulia *et al*., 2018), although the causal link between *b*-value and stress remains indirect when based on seismicity alone. Not all *b*-value minima are followed by eruptive activity, indicating that decreases in *b*-value may also reflect transient stress perturbations, magma redistribution, or aborted intrusions that do not culminate in surface eruptions. In particular, the pronounced *b*-value reductions observed between September 2021 and July 2022 were not followed by surface eruptions. Furthermore, during 2024 the temporal evolution of seismicity and *b*-value does not display sharply isolated pre-eruptive minima comparable to earlier episodes, but rather a more distributed pattern of seismic activity. This behaviour may reflect a transition towards a more hydraulically interconnected magmatic system, in which stress and magma are redistributed more efficiently across multiple pathways, reducing the development of localised pre-eruptive seismic crises. This interpretation is consistent with published geodetic and volcanological observations, although it cannot be directly tested using seismic data alone.

The temporal association between *b*-value minima and eruptive onsets (Figs. 2 and 6d), together with coeval increases in seismic rate and released energy, is consistent with recurrent changes in the seismic regime during the unrest cycle. These patterns are discussed below as being consistent with stress and/or pressure transients suggested by independent geophysical observations, while acknowledging the limitations of seismic proxies alone. Overall, the spatial–

temporal organisation of seismicity suggests an interaction between regional tectonic stresses and magmatic processes, in which magma intrusions and fault reactivation may jointly contribute to earthquake occurrence and migration patterns.

The depth distribution of hypocentres (Fig. 4) shows that most events are concentrated between 4 and 8 km, within the interval that Hrubcová *et al*. (2025) identified as the brittle–ductile transition beneath Fagradalsfjall. This boundary is commonly interpreted as a mechanically critical interface marking the transition between predominantly elastic-brittle behaviour and increasingly ductile deformation. Deeper events (10–20 km) beneath the Svartsengi area may indicate a deeper magmatic source region near the Moho, as proposed in recent structural and geophysical models (e.g. Matthews *et al*., 2024).

During pre-eruptive stages, several studies have proposed that magma accumulation at mid-crustal levels may increase stressing of the overlying brittle layer, facilitating dike ascent and fault reactivation; however, these processes are not directly quantified by the seismic catalogue analysed here.

Within this framework, the interaction between the regional transtensional stress regime and internal magmatic pressure is interpreted to produce a hybrid deformation field. This deformation pattern is expressed by extensional fracturing preferentially developing along NE–SW-oriented faults, right-lateral shear accommodated on WSW–ENE-trending structures, and the emplacement of subvertical dike intrusions that are guided by pre-existing structural weaknesses within the crust. This interpretation agrees with Jenkins *et al*. (2025), who describe the Reykjanes Peninsula as a transitional segment between oceanic ridge and continental crust, where deformation is distributed and controlled by an interconnected fault–dike network.

The successive seismic and eruptive sequences indicate that the Fagradalsfjall volcanic system is sustained by a complex, multi-level magmatic plumbing system, where different reservoirs interact dynamically over time (Sturkell 2005; Gomez-Vasconcelos, 2020).

The schematic cross-section in Fig. 3, consistent with the models of Marshall *et al*. (2024) and Matthews *et al*. (2024), depicts magma ascent through subvertical conduits connecting a mid-crustal reservoir at 7–9 km depth to a deeper magma source near the Moho (15–20 km). Fig. 3 should, therefore, be regarded as a conceptual framework integrating seismic observations with independent geophysical and petrological studies, rather than as a model directly constrained by hypocentral locations alone.

During the 2020–2024 period, the progressive activation of shallower dikes suggests a NE-ward migration of seismic activity and eruptive loci, interpreted as reflecting evolving connectivity within the magmatic system.

This interpretation is supported by published geodetic observations documenting migrating deformation sources along the Reykjanes Peninsula (Hakim *et al*., 2024), as well as by the spatial distribution of seismicity shown in Fig. 4. The 2021 crisis may represent the initial stage of renewed connectivity between deeper and shallower magma storage levels. The subsequent eruptive episodes in 2022 and 2023 are consistent with a phase of recharging and renewed pressurisation of a mid-crustal magma reservoir, while the 2023–2024 activity reflects the evolution towards a fully interconnected magmatic system capable of sustaining multiple, spatially distinct eruptive centres. Taken together, these observations suggest that magmatic migration in the Fagradalsfjall system does not proceed as a steady, unidirectional process, but rather occurs through episodic pulses of magma and volatiles that propagate both vertically and laterally, thereby modulating the regional stress field (Rubin, 1995).

The results of this study are consistent with the scenario proposed by Sigmundsson *et al*. (2022), who identified the current activity as part of a renewed magmatic rifting cycle along the Reykjanes Peninsula, similar to the one which occurred about 800 years ago. However, the present analysis adds quantitative constraints on the timing of seismic activation, *b*-value fluctuations, and energy release during the renewed rifting episode.

Hrubcová *et al*. (2025) identified, through high-resolution seismic tomography, a low-velocity anomaly between 6 and 9 km depth beneath Fagradalsfjall, interpreted as a partially molten magmatic accumulation zone. The cyclic variation in *b*-values and seismic energy documented here is consistent with recurrent activation of seismicity in the depth range where tomography suggests a low-velocity anomaly (Hrubcová *et al*., 2025), potentially linking deep and shallow processes. Similarly, Marshall *et al*. (2024) and Matthews *et al*. (2024) demonstrated that the repeated intrusions between 2021 and 2024 progressively modified the regional stress field, increasing the efficiency of magma transfer along pre-existing fractures. Altogether, these findings support a multi-reservoir, dynamically evolving magmatic system, where deformation and stress redistribution occur in a recurrent manner, leading to recurrent eruptions on multi-year timescales. Overall, the observations are consistent with an ongoing phase of renewed magmatic rifting on the Reykjanes Peninsula, as proposed by Sigmundsson *et al*. (2022), although direct quantitative comparisons with the 13th-century episode remain uncertain based on seismic data alone.

The Fagradalsfjall volcanic system currently appears to act as a primary locus for stress release along the western segment of the Mid-Atlantic Ridge in Iceland. From a geodynamic perspective, surface deformation during the recent unrest cycle is characterised by dominant NE–SW fissure opening accompanied by post-eruptive subsidence, while the mid-crust is interpreted to function as an elastic storage zone in which strain energy accumulates until critical conditions are reached. Periodic episodes of magma ascent are, then, inferred to reactivate pre-existing fault structures, leading to stress redistribution and facilitating dike propagation. Taken together, these observations suggest that the future evolution of the Reykjanes Peninsula is likely to be governed by recurring episodes of magma intrusion, seismic activity, and localised eruptions, potentially characterised by progressively shorter recurrence intervals. Such a scenario is consistent with the ongoing phase of active rift rejuvenation described by Sigmundsson *et al*. (2022), although the timing and magnitude of future events remain subject to significant uncertainty.

6. Conclusions

The analysis of seismicity and eruptive activity across the Reykjanes Peninsula between 2020 and 2024 provides a coherent picture of the recent seismo-magmatic evolution of the Fagradalsfjall volcanic system, which is interpreted, in agreement with previous geophysical and geodetic studies, as part of an ongoing phase of magmatic rifting along the western segment of the Mid-Atlantic Ridge in Iceland (Sigmundsson *et al*., 2022).

The results of this study indicate that the seismo-eruptive activity associated with the Fagradalsfjall volcanic system during the 2020–2024 period follows a recurrent temporal pattern, characterised by phases of enhanced seismicity preceding eruptive episodes and by subsequent seismic relaxation. In particular, increases in earthquake occurrence are commonly accompanied by decreases in the *b*-value, which tend to occur in temporal proximity to eruptive onsets. Although the *b*-value cannot be regarded as a direct measure of stress, its temporal fluctuations are consistent with changes in the crustal stress state inferred from seismicity patterns and have been widely interpreted as a proxy for differential stress variations in similar tectono-magmatic environments (Schorlemmer *et al*., 2005; Scholz, 2015).

The depth distribution of seismicity, interpreted in conjunction with published geophysical models, is consistent with a multi-level magmatic plumbing system involving mid-crustal storage zones and deeper magma sources that supply the eruptive system. The spatial evolution of seismic sequences and eruptive vents further reveals a progressive NE-ward migration of activity, suggesting increasing connectivity within the magmatic system and along pre-existing structural pathways of the Reykjanes fissure zone (Jenkins *et al*., 2025).

Taken together, these observations support an interpretation in which deformation and seismicity in the Reykjanes Peninsula are not controlled solely by the regional tectonic stress field, but are significantly influenced by time-dependent magmatic processes. Recurrent episodes of magma accumulation and ascent are inferred to interact with the transtensional tectonic regime, promoting episodic stress redistribution, fault reactivation, and dike propagation. From a broader geodynamic perspective, the Fagradalsfjall system appears to currently act as one of the main loci of stress release along the Icelandic segment of the Mid-Atlantic Ridge. The observed shortening of recurrence intervals between seismic crises and eruptive episodes is consistent with an ongoing phase of active magmatic rifting, which may persist in the coming years to decades, although the timing, magnitude, and spatial distribution of future intrusions and eruptions remain uncertain.

Future research should aim to enhance this methodological framework by incorporating high-resolution three-dimensional seismic tomography, real-time integration with GNSS and InSAR deformation data, and predictive modelling approaches, potentially based on machine learning techniques, to better constrain stress evolution, magmatic pressure thresholds, and magma migration pathways. Such integrated approaches will improve the capability to interpret and monitor stress-magma interactions in active rifting environments.

The approach adopted in this study, which combines a quantitative analysis of seismicity with statistical evaluation of the earthquake catalogue and geodynamic interpretation based on published studies, highlights the potential of the *b*-value as a diagnostic indicator for monitoring active volcano-tectonic systems. While the *b*-value cannot be regarded as a direct measure of stress, its temporal variability provides useful information on changes in the seismic regime that may accompany phases of magmatic unrest.

Acknowledgments. This work was presented at the 43rd National Conference of the GNGTS, held in Bologna from 11 to 14 February 2025.

REFERENCES

Büyükakpınar P., Isken M.P., Heimann S., Dahm T., Kühn D., Starke J., López Comino J.A., Cesca S., Doubravová J., Gudnason E.Á. and Ágústsdóttir T.; 2025: *Understanding the seismic signature of transtensional opening in the Reykjanes Peninsula rift zone, SW Iceland*. J. Geophys. Res.: Solid Earth, 130, e2024JB029566, doi: 10.1029/2024JB029566.

Clifton A.E. and Kattenhorn S.A.; 2006: *Structural architecture of a highly oblique divergent plate boundary segment.* Tectonophysics, 419, 27-40, doi: 10.1016/j.tecto.2006.03.016.

Darbyshire F.A., White R. and Priestley K.; 2000: *Structure of the crust and uppermost mantle of Iceland from combined seismic and gravity study*. Earth Planet. Sci. Lett., 181, 409-428, doi: 10.1016/S0012-821X(00)00206-5.

Einarsson P.; 1991: *Earthquakes and present-day tectonism in Iceland.* Tectonophys., 189, 261-279, doi: 10.1016/0040-1951(91)90501-I.

Einarsson P.; 2008: *Plate boundaries, rifts and transforms in Iceland*. JÖKULL, 58, 35-58, doi: 10.33799/jokull2008.58.035.

Fischer T., Hrubcová P., Salama A., Doubravová J., Ágústsdóttir T., Gudnason E.Á., Horálek J. and Hersir G.P.; 2022: *Swarm seismicity illuminates stress transfer prior to the 2021 Fagradalsfjall eruption in Iceland*. Earth Planet. Sci. Lett., 594, 117685, doi: 10.1016/j.epsl.2022.117685.

Gardner J.K. and Knopoff L.; 1974: *Is the sequence of earthquakes in southern California, with aftershocks removed, Poissonian?* Bull. Seismol. Soc. Am., 64, 1363-1367.

Gómez-Vasconcelos M.G. and Gudmundsson A.; 2020: *Volcanotectonics, understanding the structure, deformation, and dynamics of volcanoes*. Bull. Volcanol. 82(60), doi: 10.1007/s00445-020-01399-z.

Gulia L. and Wiemer S.; 2010: *The influence of tectonic regimes on the earthquake size distribution: a case study for Italy*. Geophys. Res. Lett., 37, 10305, doi: 10.1029/2010GL043066.

Gulia L., Rinaldi A.P., Tormann T., Vannucci G., Enescu B. and Wiemer S.; 2018: *The effect of a mainshock on the size distribution of the aftershocks*. Geophys. Res. Lett., 45(24), 13277–13287, doi: 10.1029/2018GL080619.

Gutenberg B. and Richter C.F.; 1944: *Frequency of earthquakes in California*. Bull. Seismol. Soc. Am., 34, 185-188.

Hakim W.L., Fadhillah M.F., Lee S., Park S., Baek W.-K., Hong C.-K., Kim H.-C. and Lee C.-W.; 2024: *Time-series InSAR measurement using ICOPS and estimation of along-track surface deformation using MAI during the 2021 eruption of Fagradalsfjall Volcano, Iceland*. Sci. Rep., 14, 30709, doi: 10.1038/s41598-024-79128-1.

Halldórsson S.A., Marshall E.W., Caracciolo A., Matthews S., Bali E., Rasmussen M.B., Ranta E., Gunnarsson R.J., Guðfinnsson G.H., Sigmarsson O., Maclennan J., Jackson M.G., Whitehouse M.J., Jeon H., van der Meer Q.H.A., Mibei G.K., Kalliokoski M.H., Repczynska M.M., Rúnarsdóttir R.H., Sigurðsson G., Pfeffer M.A., Scott S.W., Kjartansdóttir R., Kleine B.I., Oppenheimer C., Aiuppa A., Ilyinskaya E., Bitetto M., Giudice G. and Stefánsson A.; 2022: *Rapid shifting of a deep magmatic source at Fagradalsfjall volcano, Iceland*. Nature, 609, 529–534, doi: 10.1038/s41586-022-04981-x.

Hrubcová P., Vavryčuk V., Fischer T. and Doubravová J.; 2025: *Stress variations and non-shear earthquakes before the 2021 Iceland eruption trace magmatic fluid flow*. Commun. Earth Environ., 6, 575, doi: 10.1038/s43247-025-02533-5.

IMO (Icelandic Met Office); n.d.: https://en.vedur.is/.

Jenkins J., Greenfield T., White R.S., Maclennan J., Gudnason E.Á., Ágústsdóttir T., Rawlinson N., Obermann A., Dahm T., Milkereit C., Rahimi Dalkhani A., Fone J.W., Hersir G.P. and Doubravová J.; 2025: *Seismic imaging of the Reykjanes Peninsula, Iceland: crustal-scale context of geothermal areas and ongoing volcano-tectonic unrest*. Geochem., Geophys., Geosyst., 26, e2024GC011817, doi: 10.1029/2024GC011817.

Jonsdottir K., Cubuk Sabuncu Y., Geirsson H., Klaasen S., Caudron C., Lecocq T., Barsotti S., Barnie T., Sigmundsson F., Oddsson B., Gudmundsson M., Parks M., Fichtner A., Thrastarson S. and Paitz P.; 2021: *Seismic monitoring of the 2021 Fagradalsfjall eruption, SW Iceland*. In: Proc. AGU Fall Meeting 2021, New Orleans, LA, USA, id. V23B-05, https://ui.adsabs.harvard.edu/abs/2021AGUFM.V23B..05J.

Marshall E.W., Caracciolo A., Bali E., Halldórsson S.A., Matthews S., Ranta E., Rasmussen M.B., Robin J.G., Guðfinnsson G.H., Maclennan J., Bosq C., Auclair D., Sigmarsson O., Merrill H., Gísladóttir B., Johnson S., Löw N., Stracke A. and Genske F.; 2024: *The petrology and geochemistry of the 2021 Fagradalsfjall eruption, Iceland: an eruption sourced from multiple, compositionally diverse, near-Moho sills*. AGU Advances, 5, e2024AV001310, doi: 10.1029/2024AV001310.

Matthews S.W., Caracciolo A., Bali E., Halldórsson S.A., Sigmarsson O., Guðfinnsson G.H., Pedersen G.B.M., Robin J.G., Marshall E.W., Aden A.A., Gísladóttir B.Ý., Bosq C., Auclair D., Merrill H., Levillayer N., Löw N., Rúnarsdóttir R.H., Johnson S.M., Steinþórsson S. and Drouin V.; 2024: *A dynamic mid-crustal magma domain revealed by the 2023 to 2024 Sundhnúksgígar eruptions in Iceland*. Sci., 386, 309-314, doi: 10.1126/science.adp8778.

Mackenzie K., McClain J.S. and Orcutt J.A.; 1982: *Constraints on crustal structure in eastern Iceland based on extremal inversions of refraction data*. J. Geoph. Res., 87, 6371-6382.

Murru M., Console R., Falcone G., Montuori C. and Sgroi T.; 2007: *Spatial mapping of the b value at Mount Etna, Italy, using earthquake data recorded from 1999 to 2005*. J. Geoph. Res.: Solid Earth, 112(B12), doi: 10.1029/2006JB004791.

Parks M., Sigmundsson F., Drouin V., Hjartardóttir Á.R., Geirsson H., Hooper A., Vogfjörd K.S., Ófeigsson B.G., Hreinsdóttir S., Jensen E.H., Einarsson P., Barsotti S. and Fridriksdóttir H.M.; 2023: *Deformation, seismicity, and monitoring response preceding and during the 2022 Fagradalsfjall eruption, Iceland*. Bull. Volcanol., 85, doi: 10.1007/s00445-023-01671-y.

Rubin A.M.; 1995: *Propagation of magma-filled cracks.* Ann. Rev. Earth Planet. Sci., 23, 287-336.

Scholz C.H.; 2015: *On the stress dependence of the earthquake b value.* Geophys. Res. Lett., 42, 1399-1402, doi: 10.1002/2014GL062863.

Schorlemmer D., Wiemer S. and Wyss M.; 2005: *Variations in earthquake-size distribution across different stress regimes.* Nature, 437, 539–542, doi: 10.1038/nature04094.

Sigmundsson F., Parks M., Hooper A., Geirsson H., Vogfjörd K.S., Drouin V., Ófeigsson B.G., Hreinsdóttir S., Hjaltadóttir S., Jónsdóttir K., Einarsson P., Barsotti S., Horálek J. and Ágústsdóttir T.; 2022: *Deformation and seismicity decline before the 2021 Fagradalsfjall eruption*. Nature, 609, 523–528, doi: 10.1038/s41586-022-05083-4.

Sturkell E., Ágústsson K., Lind A., Sacks S., Einarsson P., Sigmundsson F., Geirsson H., Pedersen R. and Femina P.; 2005: *Geodetic constraints on the magma chamber of the Hekla volcano, Iceland*. In: AGU Fall Meeting 2005 Abstracts, San Francisco, CA, USA.

Uhrhammer R.A.; 1986: *Characteristics of northern and central California seismicity.* Earthquake Notes, 57, 21.

van der Elst N.J; 2021: *B-positive: a robust estimator of aftershock magnitude distribution in transiently incomplete catalogs*. J. Geophys. Res.: Solid Earth, 126, e2020JB02102, doi: 10.1029/2020JB021027.

van Stiphout T., Zhuang J. and Marsan D.; 2012: *Seismicity declustering*. Community Online Resour. Stat. Seism. Anal., doi: 10.5078/corssa-52382934.

Wiemer S. and Wyss M.; 2000: *Minimum magnitude of completeness in earthquake catalogs: examples from Alaska, the western United States, and Japan.* Bull. Seismol. Soc. Am., 90, 859-869, doi: 10.1785/0119990114.

Corresponding author: Anna Figlioli
Istituto Nazionale di Geofisica e Vulcanologia, Sezione di Milano
Via Alfonso Corti 12, 20133 Milano, Italia
Phone: +39 327 8369021; e-mail: anna.figlioli@ingv.it